LASER INTERFEROMETER GRAVITATIONAL WAVE OBSERVATORY

LIGO Laboratory / LIGO Scientific Collaboration

LIGO-T060080-00-Z *ADVANCED LIGO* 04/25/06

A Note on Optimal Spherical Approximation to Thermal Lensing

M.A. Arain, G. Mueller, D.H. Reitze, and D.B. Tanner

California Institute of Technology
LIGO Project – MS 18-34
1200 E. California Blvd.
Pasadena, CA 91125
Phone (626) 395-2129
Fax (626) 304-9834
E-mail: info@ligo.caltech.edu

Massachusetts Institute of Technology
LIGO Project – NW17-161
175 Albany St
Cambridge, MA 02139
Phone (617) 253-4824
Fax (617) 253-7014
E-mail: info@ligo.mit.edu

LIGO Hanford Observatory
P.O. Box 1970
Mail Stop S9-02
Richland WA 99352
Phone 509-372-8106
Fax 509-372-8137

LIGO Livingston Observatory
P.O. Box 940
Livingston, LA 70754
Phone 225-686-3100
Fax 225-686-7189

http://www.ligo.caltech.edu/

Table of Contents

1 Introduction

1.1 Purpose

The purpose of this note is to present a comprehensive approach for approximating non-spherical surface deformations/effects through a spherical lens approximation. A common occurrence is in the case of thermal lensing in high power cavity-enhanced interferometers.[1] The surface deformation in these cases is usually not quadratic and hence an approximation is required to represent the thermal lens by a spherical lens. Here, we present a solution to this problem by evaluating overlap integral and maximizing the power in the fundamental Gaussian mode with the thermal lens radius of curvature as a parameter to be optimized. Specific examples for the case of thermal lensing in LIGO cavities are presented. This approach also provides a quick estimation of total higher order losses due to thermal lensing.

1.2 Scope

This document is prepared for the purpose of introducing optimal estimation of radius of curvature associated with thermal lensing in optical elements. Typical readers of this include people involved in designing core optics, thermal lensing correction, alignment sensing, and material scientists.

1.3 Definitions

Thermo-optic Coefficient: Quantitative measure of the change in refractive index with temperature, represented by d*n*/d*T*.

α_t: Thermal expansion coefficient.

1.4 Acronyms

TOC: Thermo-optic coefficient

ROC: Radius of curvature

HV Theory: Hello-Vinet Theory

1.4.1 LIGO Documents

1. M. A. Arain et. al., “Thermal Compensation in Stable Recycling Cavity,” in LIGO LSC Meeting, March 2006, LIGO-G060155-00.

1.4.2 Non-LIGO Documents

2. P.Hello and J. Vinet, “Analytical models of thermal aberrations in massive mirrors heated by high power laser beams,” J. Phys. France **51**, 1267-1282, (1990).
3. P. Hello and J. Vinet, “Analytical models of transient thermoelastic deformations of mirrors heated by high power CW laser beams,” J. Phys. France **51,** 2243-2261, (1990).

2 General description

When a high power laser beam is reflected or transmitted through an optical material, a portion of the light power is absorbed in the coating or in the substrate depending upon the physical properties of the materials. This absorbed power creates a non-uniform temperature distribution on the surface and in the substrate of the material. This results in surface deformation due to the coefficient of linear expansion (α_t) of the material. Furthermore, this temperature distribution also changes the refractive index of the material depending upon the thermo-optic coefficient (TOC or dn/dT). These two effects create substantial thermal aberrations, i.e., position based optical path length change, in the reflected/transmitted optical beam. A common method is to model this behavior by introducing an imaginary lens at the surface and in the substrate. Hence, this effect is termed as thermal lensing. The focal length of this lens depends upon the geometry and physical properties of the material and the incident optical beam. However the thermal aberrations are not exactly quadratic as in the case of an ideal optical lens. The surface deformations and the thermal aberrations inside the substrate may be represented by a higher order polynomial as shown below:

$$s(x) = \sum_{n=0}^{N} A_n x^n \qquad (1)$$

Here, s(x) represents the aberration in the x direction approximated by a polynomial of order N with the coefficient of n^{th} term given by A_n. Usually s(x) is an even function so it contains only even powers of x. Generally, the coefficient of x^2 term, i.e., A_2 is used to approximate the aberrations by a perfect spherical lens. This value can vary depending upon the order of the polynomial and the type of method used to construct the polynomial. An incorrect estimation can produce unwanted higher order modes and aberrations in the system. If the optical surface is a mirror in a cavity, an optimized approximation is all the more important, because this will affect the beam size estimation as beam size is a function of radius of curvature (ROC) of the mirrors. Here, we present a general method that can be applied to estimate ROC in thermal lensing due to both surface deformation and heating in the substrate.

3 Mathematical Foundations

Consider a general situation in which an optical beam with a fundamental Gaussian TEM_{00} profile is incident on an optical surface of ROC R_1 with a minimum beam waist of w_0 at z = 0, beam waist w(z) at a distance z from the origin, and phase front radius of curvature R(z) with co-ordinate system shown in Fig. 1. Here w(z) corresponds to a fixed pre-determined value used for the hot case.

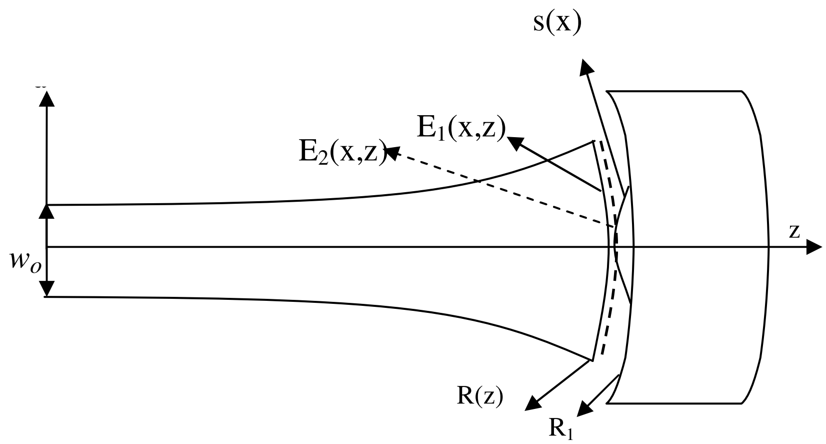

Fig. 1: Geometry of the incident and reflected electric fields from an optical material with thermal lensing.

Here $s(x)$ represents the deformation or the thermal aberration due to thermal lensing. These aberrations can be calculated by using H-V theory.[2,3] The incident electric field in the fundamental Gaussian beam is given by:

$$E_1(x,z) = \left(\frac{2}{\pi}\right)^{1/4} \frac{1}{\sqrt{w(z)}} e^{-x^2\left[\frac{1}{w^2}+i\frac{\pi}{\lambda R(z)}\right]} \tag{2}$$

The actual reflected beam from the surface is given by:

$$E_2(x,z) = \left(\frac{2}{\pi}\right)^{1/4} \frac{1}{\sqrt{w(z)}} e^{-x^2\left[\frac{1}{w^2(z)}+i\frac{\pi}{\lambda R(z)}-i\frac{2\pi}{\lambda R_1}+i\frac{\pi}{\lambda}\frac{4s(x)}{x^2}\right]} \tag{3}$$

Here $\frac{\pi}{\lambda_1}\frac{4s(x)}{x^2}$ is the optical phase difference introduced by the actual thermal lens. Now consider that the electric field $E_3(x, z)$ reflected by the imaginary perfect thermal lens with ROC of R_{opt} can be expressed as:

$$E_3(x,z) = \left(\frac{2}{\pi}\right)^{1/4} \frac{1}{\sqrt{w(z)}} e^{-x^2\left[\frac{1}{w^2(z)}+i\frac{\pi}{\lambda R(z)}-i\frac{2\pi}{\lambda R_1}+i\frac{\pi}{\lambda}4A_{opt}\right]} \tag{4}$$

Note that here we assume that A_{opt} is a parameter that is the optimized value of the coefficient used to represent the thermal lens and is equal to $A_{opt} = \frac{1}{2R_{opt}}$ where R_{opt} is the optimized ROC of the thermal lens. Note that this parameter A_{opt} is used to determine correct $w(z, A_{opt})_{cold}$ for mode matching in the cold case. In case the material under consideration is not a part of some cavity, $w(z, A_{opt})_{cold} = w(z)$ and will not depend upon the value of A_{opt} . To get an optimal value of A_{opt}, an overlap integral I is evaluated between E_2 and E_3 given by:

$$\begin{aligned} I(A_{opt}) &= \int_{-\infty}^{\infty} E_2(x,z)\times E_3^*(x,z)\,dx \\ &= \left(\frac{2}{\pi}\right)^{1/2} \frac{1}{w(z)} \int_{-\infty}^{\infty} e^{-x^2\left[\frac{2}{w^2(z)}+i\frac{\pi}{\lambda}\frac{4s(x)}{x^2}-i\frac{\pi}{\lambda}4A_{opt}\right]} dx \end{aligned} \tag{5}$$

This overlap integral represented by Eq. 5 represents the amplitude coupling from the actual reflected beam into the fundamental Gaussian mode because E_3 represents a pure fundamental Gaussian mode. This is because here the thermal lens is represented by a perfect spherical lens. The optimal value of A_{opt} is given by the maxima of the overlap integral I. This value of A_{opt} will present the optimal spherical approximation to the thermal lensing effect.

The above integral can be written as:

$$I(A)=\left(\frac{2}{\pi}\right)^{1/2}\frac{1}{w(z)}\int_{-\infty}^{\infty}e^{-x^2\left[\frac{2}{w^2(z)}\right]}e^{i\left[\frac{4\pi}{\lambda_1}s(x)-\frac{\pi}{\lambda}4A_{opt}x^2\right]}dx \qquad (6)$$

Here, using Euler's identity of $e^{i\theta}=\cos\theta+i\sin\theta$ and noting that the integral I is an even function of x, Eq. 6 can be written as:

$$I(A)=2\left(\frac{2}{\pi}\right)^{1/2}\frac{1}{w(z)}\int_{0}^{\infty}e^{-x^2\left[\frac{2}{w^2(z)}\right]}\left[\cos\left\{\frac{4\pi}{\lambda}\left(s(x)-A_{opt}x^2\right)\right\}+i\sin\left\{\frac{4\pi}{\lambda}\left(s(x)-A_{opt}x^2\right)\right\}\right]dx \qquad (7)$$

Now using Taylor's series expansion of $\cos(\theta)\approx 1-\theta^2/2$ and $\sin(\theta)\approx\theta$ near $\theta=0$, Eq. 7 can be expanded as:

$$\begin{aligned}
I(A)&=2\left(\frac{2}{\pi}\right)^{1/2}\frac{1}{w(z)}\int_{0}^{\infty}e^{-x^2\left[\frac{2}{w^2(z)}\right]}\left[1-\frac{8\pi^2}{\lambda^2}\left(s(x)-A_{opt}x^2\right)^2+i\left\{\frac{4\pi}{\lambda}\left(s(x)-A_{opt}x^2\right)\right\}\right]dx\\
&=2\left(\frac{2}{\pi}\right)^{1/2}\frac{1}{w(z)}\int_{0}^{\infty}e^{-x^2\left[\frac{2}{w^2(z)}\right]}dx-2\left(\frac{2}{\pi}\right)^{1/2}\frac{1}{w(z)}\frac{8\pi^2}{\lambda^2}\int_{0}^{\infty}e^{-x^2\left[\frac{2}{w^2(z)}\right]}\times\\
&\quad\left[A_{opt}^2x^4-2A_{opt}x^2s(x)+s^2(x)\right]\mathrm{dx}+i\times 2\left(\frac{2}{\pi}\right)^{1/2}\frac{1}{w(z)}\frac{4\pi}{\lambda}\int_{0}^{\infty}e^{-x^2\left[\frac{2}{w^2(z)}\right]}\times\\
&\quad\left[s(x)-Ax^2\right]dx\\
&=1-(I_1+I_2+I_3)+i(I_4-I_5)
\end{aligned} \qquad (8)$$

Here, Eq. 8 represents a complex integral with real and imaginary parts. The integrals I_1, I_2, I_3, I_4, and I_5 are given by:

$$I_1 = 2\left(\frac{2}{\pi}\right)^{1/2} \frac{1}{w(z,A_{opt})} \frac{8\pi^2}{\lambda^2} \int_0^\infty e^{-x^2\left[\frac{2}{w^2(z,A_{opt})}\right]} A_{opt}^2 x^4 \, dx$$

$$I_2 = -2\left(\frac{2}{\pi}\right)^{1/2} \frac{1}{w(z,A_{opt})} \frac{8\pi^2}{\lambda^2} \int_0^\infty e^{-x^2\left[\frac{2}{w^2(z,A_{opt})}\right]} 2A_{opt} x^2 s(x) \, dx$$

$$I_3 = 2\left(\frac{2}{\pi}\right)^{1/2} \frac{1}{w(z,A_{opt})} \frac{8\pi^2}{\lambda^2} \int_0^\infty e^{-x^2\left[\frac{2}{w^2(z,A_{opt})}\right]} s^2(x) \, dx \tag{9}$$

$$I_4 = 2\left(\frac{2}{\pi}\right)^{1/2} \frac{1}{w(z,A_{opt})} \frac{4\pi}{\lambda} \int_0^\infty e^{-x^2\left[\frac{2}{w^2(z,A_{opt})}\right]} s(x) \, dx$$

$$I_5 = 2\left(\frac{2}{\pi}\right)^{1/2} \frac{1}{w(z,A_{opt})} \frac{4\pi}{\lambda} \int_0^\infty e^{-x^2\left[\frac{2}{w^2(z,A_{opt})}\right]} A_{opt} x^2 \, dx$$

These integrals are solved using standard integral tables and using the series expansion of $s(x)$ in the integrals in Eq. 9. The results are summarized as:

$$I_1 = \frac{3\pi^2 w^4(z) A_{opt}^2}{2\lambda^2}$$

$$I_2 = -2\frac{\pi^2 w^4(z) A_{opt}}{2\lambda^2} \sum_{n=2}^{N} \frac{(n-1)A_n w^{n-2}}{2^{n-2}}$$

$$I_3 = \frac{\pi^2 w^4(z)}{2\lambda^2}\left[2\sum_{n=2}^{N} \frac{nA_n w^{n-2}}{2^{n-2}} \sum_{n=2}^{N} \frac{A_n w^{n-2}}{2^{n-2}} - \left(\sum_{n=2}^{N} \frac{A_n w^{n-2}}{2^{n-2}}\right)^2\right] \tag{10}$$

$$I_4 = \frac{4\pi}{\lambda} \sum_{n=2}^{N} \frac{(n-1)A_n w^n}{2^n}$$

$$I_5 = \frac{A_{opt}\pi\omega^2(z)}{\lambda}$$

Substituting the values of integrals from Eq. 10 into 8, gives the overlap integral in terms of the optimizing parameter A_{opt}.

$$I = 1 - \frac{\pi^2 w^4(z)}{2\lambda^2}\left[3A_{opt}^2 - 2A_{opt}\sum_{n=2}^{N} \frac{(n+1)A_n w^{n-2}}{2^{n-2}} + 2\sum_{n=2}^{N} \frac{nA_n w^{n-2}}{2^{n-2}} \sum_{n=2}^{N} \frac{A_n w^{n-2}}{2^{n-2}} - \left(\sum_{n=2}^{N} \frac{A_n w^{n-2}}{2^{n-2}}\right)^2\right]$$

$$+ i \times \left[\frac{4\pi}{\lambda} \sum_{n=2}^{N} \frac{(n-1)A_n w^n}{2^n} - \frac{A_{opt}\pi w^2(z)}{\lambda}\right] \tag{11}$$

Note that the cold value of w(z) is a function of A_{opt} in case if the mirror is a part of any cavity. In this situation:

$$w(z, A_{opt})_{cold} = \left(\frac{\lambda R_1}{\pi}\right)^{1/2} \left(\frac{L}{2R_1 - L}\right)^{1/4} \qquad (12)$$

where $\frac{1}{R_1} = \frac{1}{R_{hot}} - 2A_{opt}$ and L is the length of the cavity. Note that the value of R_{hot} is fixed when we specify a certain beam waist for the hot case.

Here the magnitude of the integral in Eq. 11 can easily be plotted against values of A_{opt} and a maxima can be found numerically for the magnitude of I. The corresponding value of A_{opt} will give the optimal solution to the problem. One check of the validity of the above procedure is that if $s(x) = A_2 x^2$ or a perfect spherical lens, then Eq. 11 gives exactly $A_{opt} = A_2$.

3.1 A Word of caution

Note that in using Eq. 11, there is an inherent approximation that $\left(s(x) - A_{opt}x^2\right) << \lambda$, and therefore should be used in the cases where the higher order terms in the surface deformations/thermal aberrations are relatively smaller. However, in the case of Advanced LIGO, these terms are found to be relatively stronger and hence the correct procedure is to use Eq. 6 and find a numerical solution for the maxima of the overlap integral. This value should then be used to determine the cold values of ROC. A physical meaning and a practical limit can be associated with the condition $\left(s(x) - A_{opt}x^2\right) << \lambda$ by realizing that if $\left(s(x) - A_{opt}x^2\right) > \frac{\lambda}{2}$ then incorrect interference may occur. Thus in the cases $\left(s(x) - A_{opt}x^2\right) > \frac{\lambda}{2}$, the numerical solution should be used. This procedure will be followed in the next two examples for Advanced LIGO cavities.

4 Application to Advanced LIGO

Next specific example of Advanced LIGO arm cavity is considered. We have assumed:

L = 4000 m

λ = 1064 nm

R_1=2077 m

Material= Fused Silica.

Power in Arm Cavity=850 kW

Power in Recycling Cavity = 2.1 kW

Coating Absorption = 0.5 ppm

Substrate Absorption = 2 ppm/cm

w(@ITM)=6.0 cm

Thickness of Substrate = 20 cm

Diameter of Substrate = 34 cm

4.1 Surface Thermal Lensing

Using these values, the surface deformation due to coating absorption is calculated using Hello-Vinet theory and is shown in Fig. 2. A 12th degree polynomial is used to represent the surface profile of the deformations.

Here Fig. 2 shows that a 12th degree polynomial (plotted in red) very accurately represents the surface profile plotted in cyan that is underneath the red curve. The blue curve is the approximation using the quadratic term of the 12th degree polynomial and indeed differs significantly from the actual surface. Next, the integral in Eq. 6 is evaluated for different values of A_{opt} and is plotted in Fig. 3. Here the curve shows a maxima at $1/(2\ A_{opt}) = 110.10$. Based upon this, the black curve in Fig. 2 represents the exact optimized solution to the surface profile. The green curve shows the approximation by the quadratic term of 8th degree polynomial. Some other specifications for the three cases are presented in Table 1.

It is important to note that the losses indicated in the figure are 1-D amplitude losses only. An estimate for the total losses can be made by calculating Total Losses = (1-One Dimensional Amplitude Losses)^4. Table 1 and 2 use such a value to represent the total losses.

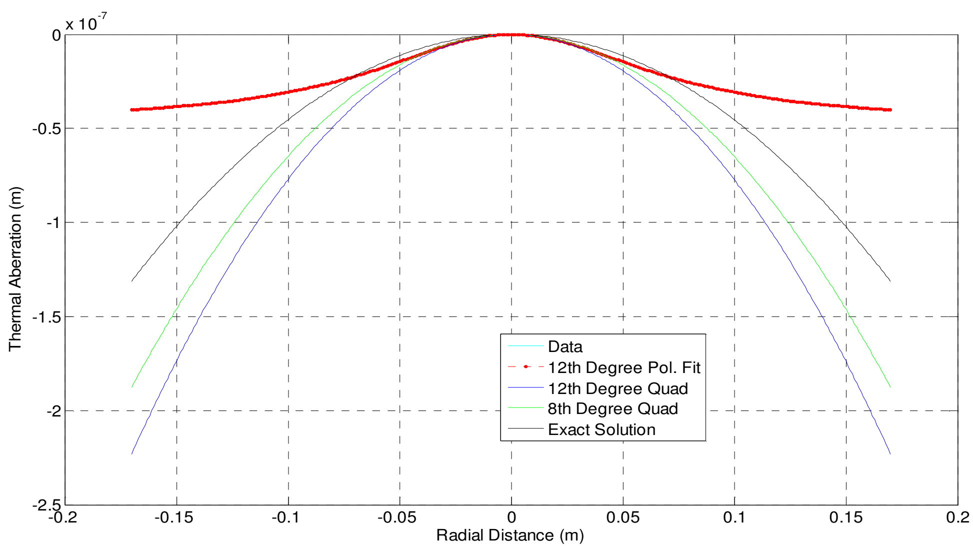

Fig. 2: Surface Thermal aberrations and their approximation by various methods in the case of surface thermal lensing.

Table 1: Summary of Optimization for Surface Thermal Lensing

Method	*Thermal ROC(Km)*	ROC_{cold} (m)	Cold Beam Size (cm)	Losses %
A_2 of 12th Pol.	64.768	2012.46	9.29	0.48
A_2 of 8th Pol.	77.013	2022.45	8.04	0.23
Exact Sol.	110.10	2038.54	7.05	0.06

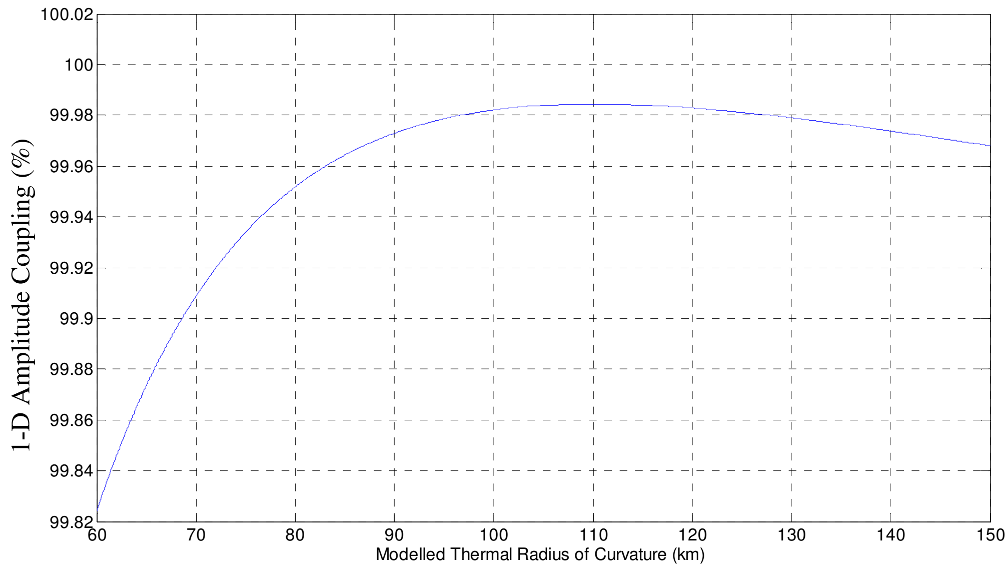

Fig. 3: Plot of 1-D amplitude coupling in the fundamental TEM_{00} mode for the case of Fig. 2.

4.2 Substrate Thermal Lensing

Next the case of thermal aberrations in substrate due to both coating absorption and substrate absorption is considered. Here, the thermal aberrations can again be approximated as thermal lens and the to be optimized parameter is the radius of curvature of that thermal lens. A similar procedure is adopted to find the exact solution. The results are summarized in Table 2, while Fig. 4 and Fig. 5 represent the thermal aberrations and the 1-D amplitude coupling in the fundamental TEM_{00} mode.

Table 2: Summary of Optimization for Substrate Thermal Lensing

Method	*Thermal ROC(Km)*	Losses %
A_2 of 12th Pol.	4.091	37.43
A_2 of 8th Pol.	4.890	21.29
Exact Sol.	5.123	10.52

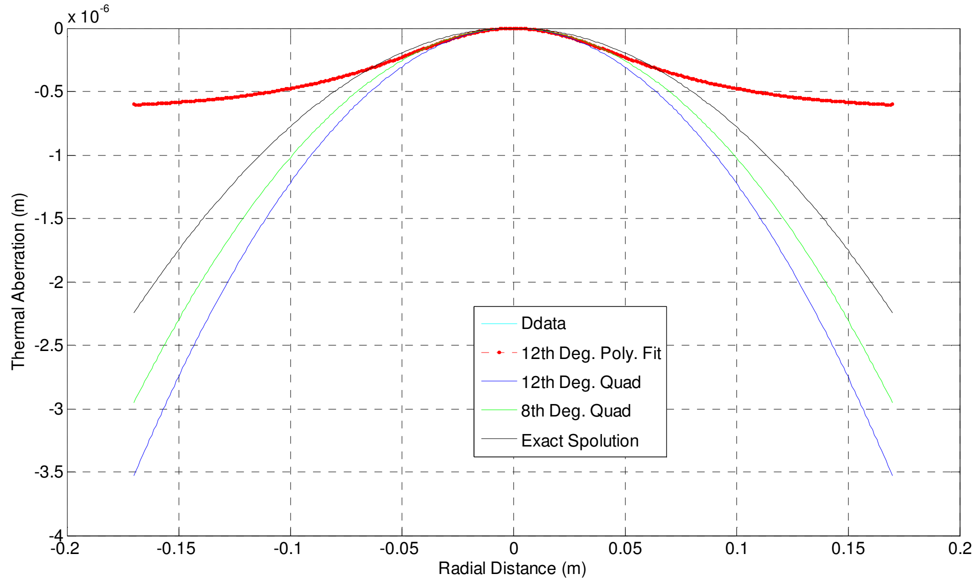

Fig. 4: Substrate thermal aberrations and their approximation by various methods in the case of substrate thermal lensing.

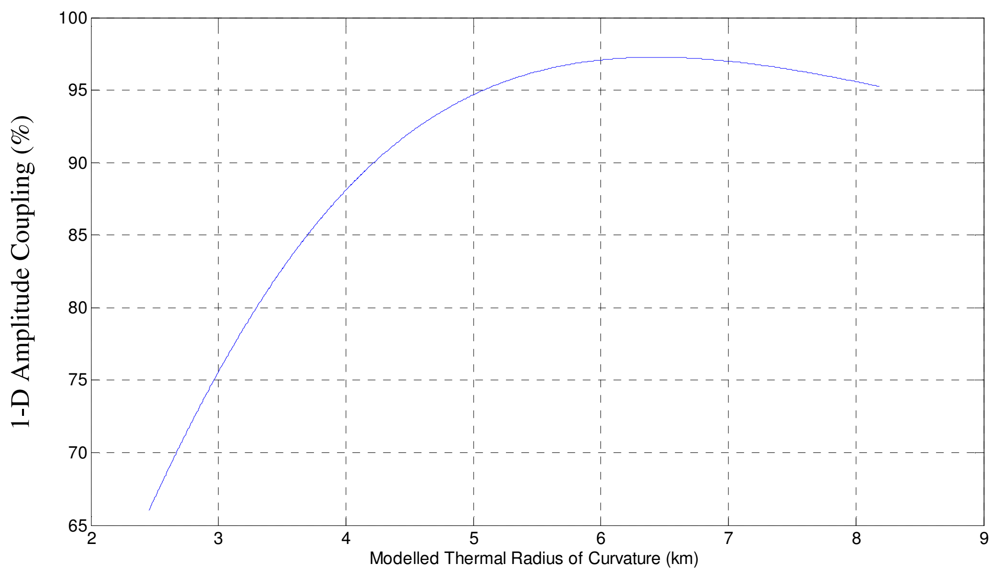

Fig. 5: Plot of 1-D amplitude coupling in the fundamental TEM_{00} mode for the case of Fig. 4.

The losses due to non-spherical nature of the thermal lensing are substantial in the case of substrate. This is somewhat expected as the thermal lensing in substrate is considerably higher as compared to the thermal lensing due to surface deformations. The absolute losses here are 11% and optimal estimation of ROC of thermal lens is very important. For example, in the case of 8th degree polynomial, the higher order losses are expected to be 21% and these losses increase to 37% in the case of 12th degree polynomial.

Another advantage of the presented approach is its ability to predict the over-all losses in the cavity due to higher order modes. Though the approach does not provide power in specific higher order modes, this does give the sum of all higher order losses.

5 Conclusion

In conclusion, a comprehensive method of approximating the real thermal aberration due to thermal lensing in optical surfaces is presented for thermal lensing effects in optical materials. The procedure involves fitting the thermal aberration with the highest possible degree polynomial and then finding an optimized value of quadratic term approximation to this solution. The overlap integral v/s the ROC is a parabola like shape and the maxima is given by the vertex of the shape. The exact solution can easily be obtained through numerical techniques. The procedure is fairly general and can be applied to a large number of problems. Furthermore, the ability to provide total higher order losses further increase the usefulness of the technique.

In Advanced LIGO, this procedure must be employed for the case of substrate thermal lensing. An incorrect estimation can result in substantial increase of higher order losses in addition to un-avoidable higher order losses of approximately 11%.